

Obtaining Explainable Classification Models using Distributionally Robust Optimization

Sanjeeb Dash, Soumyadip Ghosh, João Gonçalves, Mark S. Squillante
IBM Research, Yorktown Heights, NY 10598

November 6, 2023

Abstract

Model explainability is crucial for human users to be able to interpret how a proposed classifier assigns labels to data based on its feature values. We study generalized linear models constructed using sets of feature value rules, which can capture nonlinear dependencies and interactions. An inherent trade-off exists between rule set sparsity and its prediction accuracy. It is computationally expensive to find the right choice of sparsity – e.g., via cross-validation – with existing methods. We propose a new formulation to learn an ensemble of rule sets that simultaneously addresses these competing factors. Good generalization is ensured while keeping computational costs low by utilizing distributionally robust optimization. The formulation utilizes column generation to efficiently search the space of rule sets and constructs a sparse ensemble of rule sets, in contrast with techniques like random forests or boosting and their variants. We present theoretical results that motivate and justify the use of our distributionally robust formulation. Extensive numerical experiments establish that our method improves over competing methods – on a large set of publicly available binary classification problem instances – with respect to one or more of the following metrics: generalization quality, computational cost, and explainability.

1 INTRODUCTION

The output of many popular machine learning (ML) methods for binary classification such as random forests are hard to interpret and analyze. In many applications that have societal impact, e.g., in areas such as criminal justice and medicine, the use of ML models that are not interpretable is being questioned (Rudin, 2019; Rudin et al., 2022). In recent years, there has been a lot of emphasis on explainability and interpretability in ML models. This has led to methods such as LIME (Ribeiro et al., 2016) that explain the predictions of a classifier by approximating it locally with an interpretable model and also led to revisiting rule sets (Dash et al., 2018; Wang et al., 2017), rule lists (Lakkaraju et al., 2016), and decision trees (Hu et al., 2019) as interpretable classifiers. Ensembles of rules (i.e., linear combinations of rule outputs) are considered by Friedman and Popescu (2008) instead of rule sets (i.e., disjunctions of rules), though there is less emphasis on the sparsity of the ensemble. Dhurandhar et al. (2020) construct pre-selected interpretable ensembles of models hand-picked for explainability, and optimize the parameters of the models as well as the weights of each ensemble member by comparing their output on a training dataset to that of a good non-interpretable model. Lakkaraju et al. (2016) present a user-study that compares the ability of humans to interpret rule sets and rule lists and concludes that rule sets are more interpretable than rule lists.

In the above-mentioned papers on rules sets and decision trees, model complexity is considered an important parameter for interpretability. For rule sets, one measure of complexity (Dash et al., 2018) is the number of rules plus the number of terms in the rules. Experimental results in (Schmid et al., 2017; Muggleton et al., 2018) show that, for logic programs (which include rule sets and decision trees), inspection time (the time taken by humans to study and understand the program before applying it) is negatively correlated with human predictive performance applying the logic program. It is clear that higher model complexity will in general lead to more inspection time. Thus compact rule sets are considered to be more interpretable than

rule sets with many rules, yet the latter usually have more predictive accuracy, and so one needs to trade off model complexity and predictive accuracy. However, more complex models can lead to the overfitting of training data and subsequent poor generalization over unseen data assumed to be sampled from the same underlying (unknown) distribution. Cross-validation is used by Dash et al. (2018) to choose a good model complexity. This is computationally expensive since each training with a given complexity bound requires solving a combinatorial optimization problem.

In this paper, we focus on sparse ensembles of rule sets as binary classifiers (for binary data). These generalize both rule set classifiers and ensembles of rules (Friedman and Popescu, 2008). We define the complexity of our ensembles to be the sum of the complexities of the rule sets used in the ensemble (see Section 2.1 for a definition of rule set complexity). We limit model complexity to improve interpretability while trying to obtain more accurate classifiers than rule sets of similar complexity levels. To avoid an expensive cross-validation step to choose the appropriate model complexity and to obtain good generalization, we use a distributionally robust optimization (DRO) approach.

Recently, Ghosh et al. (2021) showed that DRO-based statistical learning solutions generalize as well as those obtained by regularized learning formulations that need computationally expensive fine-tuning via cross-validation. They provided efficient algorithms to solve DRO problems over models with continuous variables. However, their DRO formulation does not translate directly to the cases of binary-valued data and rule set models (see remarks at the end of Section 2.3). We extend this DRO approach in a couple of important ways in order to apply it to binary-valued data and rule set models.

First, we consider the selection of our classifier from the class of all *convex combinations* of rule sets. Second, we set the complexity of such a model to the sum of the complexities of the rule sets. Our formulation then selects a convex combination that is minimax optimal for a DRO formulation while satisfying a sparsity constraint. Convex combinations of binary-valued models are an important class of models that have been considered in the context of ensemble models (Sollich and Krogh, 1995), random forests (Breiman, 2001), boosting (Freund and Schapire, 1997) and their variants. These approaches have been favored by practitioners for their superior performance in out-of-training inference, and indeed they represent the state-of-the-art for many of the datasets considered in our experiments (see Section 4). However, our approach fundamentally differs from previous work in giving primary consideration to the sparsity of the chosen combination, while existing methods produce dense and hard to interpret models.

Our Contributions. We construct our sparse ensemble of rules sets using two formulations that are solved in coordination with each other. The first is a distributionally robust combinatorial optimization problem that selects a *dense* collection of *sparse* DNF classifiers that minimizes the worst loss over a carefully chosen distributional ball. The chosen DNF models obey a strict complexity bound. The solution approach utilizes column generation to efficiently search through the space of all feasible DNF models. The second smaller integer program (IP) selects a sparse *convex* combination from the dense set generated by the first formulation. This IP is easily solved with standard tools, and can be used within fine-tuning procedures to select the best complexity constraint for the chosen convex model. In Section 2, we provide upper bounds on the generalization performance of individual rule sets as well as their convex combinations in terms of their sparsity characteristics. The relevant DRO literature is reviewed in Section 2.3 and motivates the use of this approach in our algorithm, described in Section 3. In Section 4, we provide the results of our extensive experiments on binary classification models chosen from the public domain. We demonstrate that the sparse convex ensembles of rule sets we construct (a) use less computational effort than competing state-of-the-art methods; (b) while matching, and in some cases improving, the generalization performance over both the sparse rule sets of Dash et al. (2018) and the best state-of-the-art methods; and (c) are of relatively low complexity leading to easy interpretability.

2 THEORETICAL ANALYSIS

In this section we present theoretical analyses and establish related results that motivate and support our algorithm provided in Section 3. We start in Section 2.1 with establishing the notation needed to describe the problem setting and our algorithm. Section 2.2 explains why existing rule set optimization methods

require expensive computation to ensure good model generalization. Section 2.3 provides an introduction of the recent developments of DRO techniques to alleviate this concern. However, the implementation of such techniques for rule set models is complicated by the combinatorial nature of the model class. In Section 2.4, we propose the use of convex combinations of rule sets both as a more flexible model that can improve generalization and as a more suitable candidate for DRO training formulations.

2.1 Definitions

Binary classification is the problem of finding a model $F(x)$ that correctly classifies a data point x as having label $y \in \{0, 1\}$. We assume that the data x can be represented as an ordered set of d binary valued features, i.e., $x \in \{0, 1\}^d$. Data with integral or categorical features can be transformed into this setting by using, for instance, one-hot encoding. Real-valued features can be encoded in this manner by binning the range of all observed values. The true distribution P^t that generates the pair (x, y) is seldom known, and model fitting is done based on a (finite) training dataset $\mathcal{S} = \{(x_1, y_1), \dots, (x_N, y_N)\}$ of size N . We refer to $P^0 = (1/N, \dots, 1/N)$, the probability mass function (pmf) that assigns equal weights to the points in the training dataset, as the empirical pmf. The quality of a model F is determined by the loss $l(F(x), y)$ experienced at data (x, y) . In the sequel, we are interested in minimizing expected loss with respect to pmfs P over dataset \mathcal{S} : $\mathbb{E}_P l(h(x), y) = \sum_i l(h(x_i), y_i) \cdot P_i$.

Let $\mathbb{I}(\cdot)$ return 1 if its argument is true and 0 otherwise. A *simple rule* is a function of the form

$$r(x) := \mathbb{I}(x^j = 0) \text{ or } r(x) := \mathbb{I}(x^j = 1)$$

where x is a datapoint and j is an index between 1 and d . A *rule* is a conjunction $t(x)$ of simple rules and has the form

$$t(x) := r_1(x) \wedge r_2(x) \wedge \dots \wedge r_C(x),$$

or equivalently $t(x) = \prod_{v=1}^C r_v(x)$. The conjunction $t(x)$ checks if a subset of components of x have certain desired values. We also refer to each conjunction as a rule. For a fixed C , there are $\binom{2d}{C}$ such rules. A *disjunctive normal form* (DNF) classifier has the form

$$h(x) := t_1(x) \vee t_2(x) \vee \dots \vee t_M(x).$$

The DNF term $h(x)$ is often associated with the set of rules $\{t_1, \dots, t_M\}$, and thus is also called a rule set. The $h(x)$ assigns a label of 1 to x if it satisfies any of the conjunction terms t_m . This form allows the classifier to capture non-linear relationships between the features x and the label y . As an example, consider the loan application default risk classification problem from FICO (2018), where the label ‘*high risk*’ may be indicated by the disjunction of the two conjunction terms

$$(\#Loans \geq 7) \vee ((\#Loans \leq 5) \wedge (Total\ Amount \geq \$10,000)).$$

To score the explanatory power of a rule set, we associate with a conjunction $t(x)$ of C simple rules a cost $c(t) = C + 1$. The cost of a DNF term h is $c(h) = \sum_{m=1}^M c(t_m) = M + \sum_{m=1}^M C_m$.

The DNF model predicts a label $\hat{y} = h(x)$ at data point x . Dash et al. (2018) construct *sparse* rule sets with a constraint on their complexity $c(h) \leq \mathfrak{C}$. Let $\mathcal{H}(\mathfrak{C})$ denote the space of all DNF rule sets that obey this constraint. Then, for a given \mathfrak{C} , the rule set is constituted from a possible $\sum_{c=1}^{\mathfrak{C}-1} \binom{2d}{c}$ conjunction rules.

A convex combination of rule sets takes the form $F(\cdot) = \sum_k v_k h_k(\cdot)$ where each $h_k(x)$ is a rule set and the non-negative v_k satisfy $\sum_k v_k = 1$. It predicts labels by applying a threshold: $\hat{y} = \mathbb{I}(F(x) \geq 1/2)$. The cost associated with F is the sum of the individual costs $c(F) = \sum_k c(h_k)$.

2.2 Analyzing Rule Sets

The standard approach to finding a good learning model is to minimize the expected loss under the empirical pmf P^0 over the training dataset \mathcal{S} . Sparse rule sets are constructed by the optimization formulation:

$\min_{h \in \mathcal{H}(\mathfrak{C})} \mathbb{E}_{P^0} l(h(x), y)$, where the loss is $l(h(x), y) = |h(x) - y|$ to reflect the impact of $\hat{y} \neq y$. The following result sheds light on the expected gap in performance of any model on the (unknown) true data distribution P^t and P^0 .

Proposition 1. *Let P^t be the underlying distribution and P^0 the empirical pmf over a training set \mathcal{S} of size N , and the loss is measured as $l(h(x), y) = |h(x) - y|$. Then, for any $\delta \in (0, 1)$, there exists constants such that for all rule sets h with max-complexity $c(h) \leq \mathfrak{C}$, we have with probability at least $1 - \delta$:*

$$\mathbb{E}_{P^t}[l(h(x), y)] \leq \mathbb{E}_{P^0}[l(h(x), y)] + \left(\frac{2}{N} \left((\mathfrak{C} - 1) \log \frac{2d}{\mathfrak{C} - 1} + \log \frac{1}{\delta} \right) \right)^{\frac{1}{2}}. \quad (1)$$

Note that, for binary output $\hat{y} = h(x)$, $\mathbb{E}_P l(h(x), y) = \mathbb{E}_P |\hat{y} - y| = \mathbb{P}_P[\hat{y} \neq y]$. Detailed expressions on the dependence of the rate on δ are provided in the proof presented in Section A of the supplement, which extends the Vapnik-Chervonenkis bounds from Golea et al. (1997) and Schapire et al. (1998). The misclassification losses under the true distribution P^t and the empirical distribution P^0 represent the test and training performance of a model, respectively. The typical learning approach chooses an optimal model that minimizes the training error, the first term in the upper bound (1) on the test error. However, the second term is independent of the particular model chosen and grows as $O(\sqrt{\mathfrak{C}})$ for a given dataset, i.e., with fixed N . This explains the phenomenon observed in the results of Dash et al. (2018) that optimal rule sets satisfying a higher complexity \mathfrak{C} constraint can reduce the training error to zero but do not generalize as well as lower complexity solutions.

In learning settings where the models are parametrized with variables that take values in a continuous space, the standard approach to alleviate this generalization issue is to regularize the parameter value of the chosen model in an l_p norm to enforce some form of sparsity. Rule sets lack such a regularizable parameter, but sparsity can be directly enforced by the right choice of \mathfrak{C} . Dash et al. (2018) employ cross-validation to achieve this, but at the expense of a large computational cost since the procedure involves repeatedly solving a complex combinatorial minimization problem.

2.3 DRO for Learning

DRO has emerged recently (Namkoong and Duchi, 2017; Blanchet et al., 2019a; Lam and Zhou, 2017) as an alternative new statistical model training technique with rigorous foundations to establish its ability to produce models with improved generalization. Moreover, Ghosh et al. (2021) show that these formulations can be solved to produce models of similar or higher generalization quality on a significantly lower computational budget.

More specifically, DRO methods have been developed to handle the case where models are parametrized with θ , a continuous-valued variable. Let $l(\theta, \xi)$ provide a loss value for the task at hand (classification, regression, and so on) with model parameter θ at data ξ . As before, we are given an N -sized training dataset \mathcal{S} of ξ values. The DRO approach selects the model parameter that minimizes the *robust loss* $R(\theta)$:

$$\min_{\theta} \left\{ R(\theta) := \max_{P \in \mathcal{P}} \mathbb{E}_{\xi \sim P} l(\theta, \xi) \right\}$$

where $\mathcal{P} := \{P \mid D_{\phi}(P, P^0) \leq \rho, \sum_i P_i = 1, P_i \geq 0\}$.

The robust loss $R(\theta)$ is the worst loss observed for the model parameterized with θ over a set \mathcal{P} of probability vectors representing weights over the training dataset \mathcal{S} . This set \mathcal{P} is centered at the empirical pmf P^0 and allows all weights that are within a ϕ -divergence distance $D_{\phi}(\cdot, \cdot)$ of ρ from P^0 . The ϕ -divergence distance function on the space of weights is defined as $D_{\phi}(P', P) := \mathbb{E}_P \left[\phi \left(\frac{dP'}{dP} \right) \right]$, where ϕ is positive, convex and $\phi(1) = 0$. Members of this class of distance functions include the modified χ^2 divergence, with $\phi(s) = (s-1)^2$, and the Kullback-Leibler (KL) divergence, with $\phi(s) = s \log s - s + 1$.

Lam and Zhou (2017) show that, for well chosen ρ , the set $\{\arg \min_{\theta} \mathbb{E}_P l(\theta, \xi), P \in \mathcal{P}\}$ contains the minimizer of the expectation under the true data distribution P^t with high probability, even if P^t itself does not belong to \mathcal{P} . Namkoong and Duchi (2017) (Section 3.1) consider the DRO formulation with a loss convex in θ and a χ^2 -divergence uncertainty ball with radius $\rho = O(\mathfrak{V}/N)$, where \mathfrak{V} is the (finite) *Vapnik-Chervonenkis* (VC) dimension of the class of models parametrized by θ . They show that, with high probability, the robust loss $R(\theta)$ is bounded above by

$$R(\theta) \leq \mathbb{E}_{P^0} l(\theta, \xi) + (1 + o(1)) \sqrt{\frac{\mathfrak{V}}{N} \text{Var}_{P^0} l(\theta, \xi)},$$

where Var_{P^0} is the variance of the loss function with respect to the empirical pmf P^0 and we follow the notation that a function $g(v) = o(v)$ if $g(v)/v \rightarrow 0$ as $v \rightarrow \infty$. This upper bound is a close first order approximation of the right hand side of (1). (The VC dimension of the DNF rule set class of complexity up to \mathfrak{C} in (1) is \mathfrak{C} .) Thus, the model that minimizes the robust loss stands to generalize better over unseen data, given the relation (1), and does not require extensive fine tuning via heuristics like cross-validation. The experimental evidence over a large set of (convex) classification examples provided by Ghosh et al. (2021) bears this out in practice.

The development of this DRO theory motivates the consideration of an analogous formulation for rules sets, that of minimizing the robust loss of a rule set:

$$R(h) = \max_{P=(P_i) \in \mathcal{P}} \left\{ \mathbb{E}_P l(h(x), y) \right\},$$

where, as before, the function $l(h(x), y) = |\hat{y} - y|$ measures the penalty incurred when $\hat{y} = h(x) \neq y$. This formulation, however, can lead to undesirable behavior because the misclassification loss l only takes two values. The solution $P^*(h) = \arg \max_{P \in \mathcal{P}} \mathbb{E}_P l(h(x), y)$ correspondingly has a simple structure, partitioning the dataset \mathcal{S} into two subsets of the correctly classified and the misclassified, each with the same probability assigned within its members. This is quite uninformative and easily leads to cycling when solving the minimax formulation in alternating iterations over h and P : subsequent iterations of corresponding experiments where P is updated were quickly observed to cyclically over- and under-emphasize the same subsets. (Additional details and results are provided in Section 4.1.)

2.4 Ensemble Rule Sets

The issue in not being able to directly adapt DRO formulations developed for continuously valued parameter models to rule set optimization lies in the discrete nature of the models. An extensive literature has emerged in the past two decades on developing stronger models by taking linear combinations of binary models; these include ensembling models (Sollich and Krogh, 1995), such as AdaBoost (Freund and Schapire, 1997) and their variants, and an extended treatment is available for collections of rule-set like decision trees such as random forests (Breiman, 2001).

We refine the generalization result in Proposition 1 for individual rule sets to their convex combinations.

Proposition 2. *For any convex rule set combination $F = \sum_k v_k h_k$, define $\mathfrak{C}' := \max_k \{c(h_k)\}$ to be the maximum complexity of its constituent conjunctive terms, and let the predicted label be $\hat{y} = \mathbb{I}(F(x) \geq 1/2)$. Then, for any given $\delta \in (0, 1)$, with probability at least $1 - \delta$, we have*

$$\mathbb{P}_t(L(F, x, y) \leq 0) \leq \mathbb{P}_0(L(F, x, y) \leq \Delta) + O\left(\frac{1}{\sqrt{N}} \left(\frac{(\mathfrak{C}' - 1)}{\Delta^2} \log N + \log \frac{1}{\delta}\right)^{1/2}\right).$$

The proof of Proposition 2, along with expanded expressions of the rate displaying its dependence on δ , is given in Section A of the Supplement. This result shows that convex combinations of rule sets enjoy an important advantage over a single rule set; the generalization penalty (the second term) grows only with the largest complexity of its constituents, while allowing for extra *continuous* parameters (the v_k) to minimize

the training error (the first term). Hence, for a fixed complexity budget, convex combinations of rule sets can significantly improve training performance over single rule sets while displaying the generalization performance of its largest constituent rule set.

Importantly, the introduction of the continuous parameters now alleviates the binary loss issue faced in implementing DRO training of rule sets, since the *margin* of misclassification takes (depending on the v_k) more informative values. We modify the loss function to highlight this margin, and for a given datapoint x and its label y set it as

$$l(F(x), y) = \left| \sum_k v_k h_k(x) - \frac{1}{2} \right| \cdot \mathbb{I}(\hat{y} \neq y). \quad (2)$$

The algorithm presented in the next section advocates for a DRO approach of training convex combinations of rule sets with the loss function (2).

3 ENSEMBLING ALGORITHM

We now present our algorithm for identifying the optimal sparse convex DNF combination $F(x)$. Its task is divided into two optimization formulations that are solved in sequence. The first identifies a collection of good DNF models using a distributionally robust combinatorial formulation. The DNF models considered are constrained to be of complexity less than or equal to \mathfrak{C}' . The second formulation subsequently selects an optimal sparse convex combination of DNF models from the identified collection. This formulation enforces that convex combinations of only $\lfloor \mathfrak{C}/\mathfrak{C}' \rfloor$ DNF models are considered, where \mathfrak{C} is the user-desired sparsity parameter.

3.1 DRO-Based Collection of Rule Sets

The aim of this DRO formulation is to select a collection $F(x) = \sum_n (1/n) \cdot h_n(x)$ of DNF models $h_n(\cdot)$ that minimizes the robust loss objective:

$$R(F) = \max_{P \in \mathcal{P}} \{ \mathbb{E}_P l(F(x), y) \}, \quad (3)$$

where the probability ball \mathcal{P} is centered at P^0 and admits all probability mass functions $P = (P_i)$ that are a distance $D_\phi(P, P^0)$ of $\rho > 0$ from P^0 . The loss objective is as given in (2). Note that the collection gives equal weight to its constituent DNF models.

The formal distributionally robust approach to constructing an optimal collection consists of solving for $\min_F R(F)$ over all collections of any arbitrary size. The feasible space of this formulation allows for a countably infinite collection of DNF models, and is hard to search over. A similar problem has been addressed in the ensembling literature using efficient approximations. For instance, Friedman et al. (2000) show that the AdaBoost algorithm for growing ensembles of models can be viewed as a greedy approach to solving a generalized loss minimization problem over the set of all ensembles for a specific global loss objective. Moreover, Blanchet et al. (2019b) show that this generalized loss objective for AdaBoost can itself be written as a robust objective function of the form (3).

This motivates the following sequential approach to growing the collection using a greedy addition of one new DNF member in each iteration. We start with the initial weights P^0 as the empirical (equal weights) pmf and set the initial collection of DNF models to be empty, i.e., $F_0(x) = 0$. Then, in each iteration indexed by $n = 1, \dots$, we have the following steps.

1. Solve for

$$h_n := \arg \min_{h \in \mathcal{H}(\mathfrak{C}')} \mathbb{E}_{P^{n-1}} l(h(x), y). \quad (4)$$

2. Add h_n to collection:

$$F_n(x) \leftarrow \frac{n-1}{n} F_{n-1}(x) + \frac{1}{n} h_n(x).$$

3. Solve for the robust loss maximizing pmf

$$P^n := \arg \max_{P \in \mathcal{P}} \mathbb{E}_P l(F_n(x), y). \quad (5)$$

In each iteration, a new DNF model is selected that minimizes the misclassification loss over \mathcal{S} as weighted by the worst-case pmf P^{n-1} . The DNF loss function of $l(h) = |h(x) - y|$ is used in (4). This DNF model is then added to the collection. The last step then refreshes the worst pmf by maximizing for the robust loss of the current collection $F_n(x)$, using the form (2).

Column Generation for (4): This formulation searches over the (exponentially large) space $\mathcal{H}(\mathcal{C}')$ of rule sets. We follow the approach of Dash et al. (2018) to efficiently explore this space using a column generation reformulation, and extend their approach to the general case where the data weights are any arbitrary pmf P^{n-1} . Let K be the set of all possible rules. For each $k \in K$, let Z_k be the set of indices of data points with label 0. For each data index i , let K_i be the set of indices k such that rule k is satisfied by data point x_i . Let c_k be the complexity of rule k . We then solve the formulation

$$\min \sum_i \xi_i + \sum_{k \in K} \sum_{i \in Z_k} P_i w_k \quad (6)$$

$$\text{s.t. } \xi_i + P_i \sum_{k \in K_i} w_k \geq P_i, \quad \xi_i \geq 0, \quad (7)$$

$$\sum_{k \in K} c_k w_k \leq C, \quad w_k \in \{0, 1\}, \quad k \in K. \quad (8)$$

The formulation chooses a set of rules (given by nonzero values of w_k) that does not minimize the 0-1 loss but instead a weighted Hamming loss: for each data point x_i with label 1, ξ_i provides the exact loss weighted by P_i , while the second objective term with P_i values set to 1 provides the number of rules in the chosen rule set that give incorrect values to 0 label data points. Since the number of rules is exponential in number, we solve this formulation via column generation as in (Dash et al., 2018) except that terms in the dual constraints for the LP relaxation of (6) – (8) are scaled by the values P_i . Section B in the Supplement provides further details on the column generation method.

Solving for worst case pmf in (5): The objective function of (5) is expressed as $\sum_{i \in \mathcal{S}} l(F_n(x_i), y_i) \cdot P_i$, where the individual loss values $z_i = l(F_n(x_i), y_i)$ are constructed as per (2). The z_i take values in the discrete set $\{0, 1/n, \dots, 1\}$, and so as the iterations n grow, the issue noted in Section 2.3 is progressively alleviated. The formulation (5) can be equivalently written as the concave problem:

$$R(F_n) = \max_{P=(P_i) \in \mathcal{P}} \sum_{i \in \mathcal{S}} P_i z_i \quad (9)$$

$$\text{s.t. } \sum_{i \in \mathcal{S}} \phi(NP_i) \leq N\rho, \quad \sum_{i \in \mathcal{S}} P_i = 1, \quad P_i \geq 0.$$

Here, the first constraint represents the restriction on the ϕ -divergence $D_\phi(P, P^0)$ being within ρ . The objective of (9) is linear in the variable P and the constraints are convex, thus rendering a concave program. Ghosh et al. (2021) utilize Lagrangian methods to provide an algorithm that can solve this formulation efficiently. The details of this formulation are provided in Section C of the supplement. We close this description by adapting a result from Ghosh et al. (2021) for a worst-case bound on the computational effort required to obtain an ϵ -optimal solution to (9).

Proposition 3 ((Ghosh et al., 2021, Proposition 2)). *For any ϕ -divergence, the algorithm in Section C finds a feasible solution (\tilde{P}^*) to (9) with an objective function value \tilde{R} such that $|R(F) - \tilde{R}| < \epsilon$ with a worst-case computational effort bounded by $O(N \log N + (\log \frac{1}{\epsilon})^2)$, where ϵ is a small precision parameter.*

3.2 Selecting Sparse Convex Ensembles

The formulation in the previous section sequentially generates a collection $\{h_k(x), k = 1, \dots, n\}$ of DNF models each of which are the optimal solutions to minimizing the expected loss under a sequence of worst-case pmf values P^n . Each h_k has been further chosen such that their maximum complexity is at most \mathfrak{C} . We now address the question of selecting an optimal sparse convex combination (or weighted ensemble) from within this collection.

As defined in Section 2.4, the misclassification loss (2) of the convex combinations measures the margin of misclassification of \hat{y} . The optimal sparse convex combination $\sum_{k=1}^n v_k h_k$ is then determined by solving

$$\min_{v_k} \mathbb{E}_P l\left(\sum_{k=1}^n v_k h_k(x), y\right) \quad \text{s.t.} \quad \sum_{\{k \mid v_k > 0\}} c(h_k) \leq \mathfrak{C}. \quad (10)$$

This formulation is solved after every iteration of the collection-growing formulation is finished. The data weight vector used in (10) can be P^n , the worst-case pmf of the current iteration. The performance of this formulation does not seem to be sensitive to this choice of P^n in our experiments of Section 4; and a selection of $P = P^0$, the initial empirical distribution, produces similar results. (Additional details and discussion of this issue are provided in Sections C and D of the supplement.) The complexity parameter \mathfrak{C} represents the user desired complexity of the overall classifier output by our method. Section 4 further discusses how \mathfrak{C}' should be set, and also addresses the case where both parameters \mathfrak{C} and \mathfrak{C}' can be set adaptively.

We turn our attention to solving (10) efficiently. Let \mathcal{S}^0 and \mathcal{S}^1 be the subsets of the training data indices that represent data labeled with $y = 0$ and $y = 1$, respectively; so, $\mathcal{S}^0 \cup \mathcal{S}^1 = \mathcal{S}$. For each data index i , let \mathcal{K}_i represent the set of all DNF models that provide a value of 1 at x_i : $\mathcal{K}_i = \{k \mid h_k(x_i) = 1, k = 1, \dots, n\}$. Define auxiliary variables ξ_i for each data index i to represent the amount by which the data is misclassified. We then rewrite the problem (10) as the IP:

$$\min_{\xi_i^0, \xi_i^1} \sum_{i \in \mathcal{S}^0} p_i \xi_i + \sum_{i \in \mathcal{S}^1} p_i \xi_i \quad (11)$$

$$\text{subject to:} \quad \sum_{k \in \mathcal{K}_i} v_k \leq \frac{1}{2} - \Delta + \xi_i, \quad \forall i \in \mathcal{S}^0, \quad (12)$$

$$\xi_i + \sum_{k \in \mathcal{K}_i} v_k \geq \frac{1}{2} + \Delta, \quad \forall i \in \mathcal{S}^1, \quad (13)$$

$$v_k \in [0, 1], \quad \sum_k v_k = 1, \quad \xi_i^0, \xi_i^1 \geq 0,$$

$$v_k \leq w_k, \quad w_k \in \{0, 1\}, \quad \sum_k w_k c(h_k) \leq \mathfrak{C}. \quad (14)$$

The constraints (12) and (13) define the magnitude of the misclassification margin for each data index i using the auxiliary variables ξ_i , depending on by how much the threshold of 1/2 is breached for each label type. Note that an extra parameter Δ is introduced to strictly separate the two data subsets. Our experiments in Section 4 show that a small separation parameter, e.g., $\Delta = \mathfrak{C}' / (2 \cdot \min_k c(h_k))$, suffices. The binary variables w_k are introduced in (14) to enforce the maximum allowed complexity of the chosen convex combination weight values $v_k \in [0, 1]$, $\sum_k v_k = 1$.

The formulation (11) is a relatively small IP with only as many binary variables as the number of DNF models h_k in the current collection. In Section 4, we present an adaptive procedure for implementing our algorithm that solves this IP formulation a few times after each iteration of the collection-growing formulation of Section 3.1 in order to adaptively identify the best sparse convex combination to return.

4 NUMERICAL EXPERIMENTS

We follow the numerical experiments conducted by Dash et al. (2018) in evaluating their column-generation based sparsifier and conduct tests on seven classification datasets from the UCI repository (Lichman, 2013). In addition, we use the dataset from the FICO Explainable Machine Learning Challenge (FICO, 2018), which contains 23 numerical features of the credit history of 10,459 individuals (9,871 after removing records with all entries missing) for predicting repayment risk (good/bad). Section D of the supplement provides additional details on the various datasets and how they were pre-processed.

Table 1: (Middle-Left Four Columns:) Classification Performance over Unseen Test Data of Models Created by Four Competing Methods for Seven UCI Repository Datasets and the FICO Dataset. (Middle-Right Three Columns:) Complexity of Models Constructed by the Three Explainable Methods. (Last Column:) Run-Length (number of iterations n) of DR Method. All Results presented with a Mean and a 95% Confidence Interval.

Dataset Name	Test Performance (%)				Model Complexity			n , Number Iterates
	DR	CG	CART	RF	DR	CG	CART	
heart	81.5(1.7)	78.9(4.7)	81.6 (4.7)	82.5(1.4)	26.0(2.7)	11.3 (3.5)	32.0(15.9)	35.7(3.6)
ILPD	69.1(1.1)	69.6 (2.4)	67.4(3.1)	69.8(1.0)	13.3(2.3)	10.9 (5.3)	56.5(21.4)	27.0(1.8)
FICO	72.1 (0.3)	71.7(1.0)	70.9(0.6)	<u>73.1</u> (0.2)	25.0(2.5)	13.3 (8.0)	155.0(53.9)	33.9(3.3)
ionosphere	93.3 (1.4)	90.0(3.5)	87.2(3.5)	<u>93.6</u> (1.4)	20.3(2.9)	12.3 (5.9)	46.1(8.2)	38.9(4.0)
liver	58.6(1.6)	59.7 (4.7)	55.9(2.7)	<u>60.0</u> (1.6)	29.3(1.4)	5.2 (2.4)	60.2(30.6)	38.5(3.2)
pima	74.6 (1.4)	74.1(3.7)	72.1(2.5)	<u>76.1</u> (1.6)	25.0(2.8)	4.5 (2.5)	34.7(11.4)	34.5(3.6)
transfusion	78.4(0.8)	77.9(2.7)	78.7 (2.2)	<u>77.3</u> (0.6)	14.3(1.3)	5.6 (2.4)	14.3(4.5)	30.2(3.1)
WDBC	95.5 (0.5)	94.0(2.4)	93.3(1.8)	<u>97.2</u> (0.4)	28.3(1.9)	13.9 (4.7)	15.6(4.3)	36.8(3.9)

Our procedure to identify the best sparse convex combinations of DNF models implements our above algorithm by adaptively determining the best values for the complexity parameters \mathfrak{C}' (from (4)) and \mathfrak{C} (from (10)). The generalization result in Proposition 2, bolstered by our expanded set of results in Section 4.2, shows that setting a low value for \mathfrak{C}' grants more generalization flexibility to the sparse ensembling formulation (10), and so we set $\mathfrak{C}' = 5$ throughout the results of this section. The two formulations are then solved sequentially in iterations $n = 1, \dots$ as follows.

1. Solve the DRO rule set formulation (4) using the column-generation approach to identify an additional member to be added to the collection $\{h_k, k = 1, \dots, n\}$ of good DNF models; each model has complexity $c(h_k) \leq \mathfrak{C}'$. Then solve the maximization formulation (5) to obtain the pmf P^n that maximizes robust loss.
2. Solve the sparse convex combination formulation (10) in the IP form (11) – (14) for increasing values of $\mathfrak{C} = m \cdot \mathfrak{C}'$ with $m = 2, \dots$. Stop when the value of the identified optimal solution does not decrease beyond a given threshold.

The inner iterations in Step 2 are cutoff when $\mathfrak{C} = 30$. The outer iterations n are stopped when the optimal solution returned by the second step does not improve significantly over 20 successive iterations. We set the improvements threshold to show 0.5% or more change. The dataset weights used in (10) are set to the empirical (equal weights) pmf P^0 .

Implementation Details. We implement the procedure described above in Java, and use version 22.1 of the commercial solver IBM ILOG CPLEX to solve the linear programs and mixed-integer linear programs. Our column generation implementation is an extension of the approach described in Dash et al. (2018) and we refer to that paper for more details. The main parameters of the implementation are a time limit on the solution of the pricing problem in each iteration, which we set to 30 seconds, a second time limit on the overall

column generation process, which we set to 300 seconds, and a limit on the number of column generation iterations, which we set to 5. We set the DRO parameter ρ to 0.05 as measured using χ^2 -divergence for the distance function $D_\phi(P, P^0)$. The value of the parameter ρ is chosen to match the recommendation of $O(\mathfrak{C}/N)$ from Namkoong and Duchi (2017) for continuous convex learning settings. The implementation of the sparse convex combination IP formulation (11) – (14) limits the time spent in the solver to 600 seconds.

The results presented here are based on splitting each input dataset uniformly at random into a training dataset, containing 70% of the data, and a test dataset with the remaining 30% of the data. The implementation then uses the training dataset to execute the sequence of our two formulations and obtain the set of final rules, which is followed by evaluating the performance of those rules on the test dataset and reporting the results. A total of 20 such permutations are considered to produce the confidence intervals presented.

Competing Methods. We compare the test performance of our DRO-based rule set induction approach (DR) with the sparse rule set algorithm (CG) proposed by Dash et al. (2018). In addition, we include results for two decision tree models presented in (Dash et al., 2018): the CART method (Breiman et al., 1984) and the random forest RF method (Breiman, 2001). The latter method produces dense ensembles of decision trees and is not appropriate from the explainability point of view, but often produces models with good generalization for comparison.

Table 1 provides both the test accuracy and the complexity of the models identified by the various methods. For both these sets of results, the method with the best average outcomes among interpretable models is highlighted in **bold** and the best average outcome overall is underlined. Any method with average outcomes within the confidence interval of the overall best outcome is highlighted in *italics*.

The results in Table 1 (middle-left) show that DR comes close to and in half of the eight cases even exceeds the generalization performance of the competing explainable models CG and CART. Moreover, the solution quality of DR is statistically comparable to the non-interpretable RF method, which produces the best results in all but one dataset (transfusion). In fact, across all the datasets, the mean performance of the DR method lies within the confidence intervals of the overall best method, thus either representing the best method or statistically identical to the best method.

We also compare the complexity of the models from our DR approach with those obtained by three of the methods; the omitted RF method produces a dense ensemble with orders of magnitude higher complexity and is not appropriate for creating interpretable models. The results in Table 1 (middle-right) show that the complexity of the estimated models from DR is within a reasonable range of the CG method, even statistically identical in one case (ILPD), while consistently better than CART and often significantly so. These results illustrate the efficacy predicted in Proposition 2, in that sparse convex mixtures of $\mathfrak{C}' = 5$ rule sets have greater flexibility in reducing training error and simultaneously keep a low generalization gap. In contrast, the individual rule sets produced by the CG method use higher complexity than 5 to obtain a reasonable balance between reduced training error and lower test efficacy, but overall do not perform as well on test data as the convex combinations generated by DR. While the CG method may improve its training power with a higher \mathfrak{C} bound, it may suffer a higher generalization gap as shown in Proposition 1. Hence, it is not readily clear that the gap in test performance can be closed for any value of \mathfrak{C} by the CG method.

The last column also shows how many iterations of the DR method were required to attain the corresponding results. Note that each iteration contains one call to solve the expensive formulation (4). These results compare very favourably with the order of hundreds of calls to similar model estimation formulations required by the cross-validation based fine tuning of parameters of the competing methods. For example, CG solves 150 of a similar combinatorial optimization formulation with the aid of their column generation approach.

Additional results are provided below in Section 4.2 and in the supplement where the parameters chosen in this section are varied. A larger sparse mixture complexity cutoff of 60 is considered and, as can be expected, this slightly improves the generalization performance at the expense of more complex (and harder to interpret) models. Results for a larger DRO parameter $\rho = 0.5$ are presented, largely illustrating that this value makes the DRO formulation too conservative. Parameters of the stopping criteria are also varied to show that with a higher computational budget, slightly higher quality solutions can be obtained by DR for the same complexity cutoff of 30.

4.1 Cyclical Behavior of DRO for DNF Models

We noted in Section 2.3 that basing the performance on the misclassification losses $l(h(x), y) = |h(x) - y|$ can lead to undesirable cyclical behavior. This is because l takes only two values $\{0, 1\}$, and thus the solution $P^*(h) = \arg \max_{P \in \mathcal{P}} \mathbb{E}_P l(h(x), y)$ is correspondingly degenerate, partitioning the dataset \mathcal{S} into two subsets of the correctly classified and the misclassified. The data points in each of the two subsets are assigned the same probability. The subset over which $l(h(x), y) = 1$ has a large value (since all points in this subset are misclassified) and the points where the loss is zero have a small, possibly zero, probability (since all points in this subset are correctly classified). This is quite uninformative and easily leads to cycling when solving the minimax formulation in alternating iterations over h and P , in that subsequent iterations in which P is updated can cause the same two subsets of points to exchange loss values of 0 and 1, and thus the same subsets are over- and under-emphasized in a cyclical manner. This phenomenon is demonstrated in Figure 1, which presents results from solving the DRO formulation of minimizing the robust loss objective $R(h)$ defined in Section 2.3. A simplified version of the heuristic presented in Section 3.1 was implemented to solve this formulation: Step 2 of growing the collection of DNF models was omitted and in Step 3, we solve for the worst-case solution $P^*(h_n)$ that maximizes the weighted expected loss of the current DNF iterate h_n only.

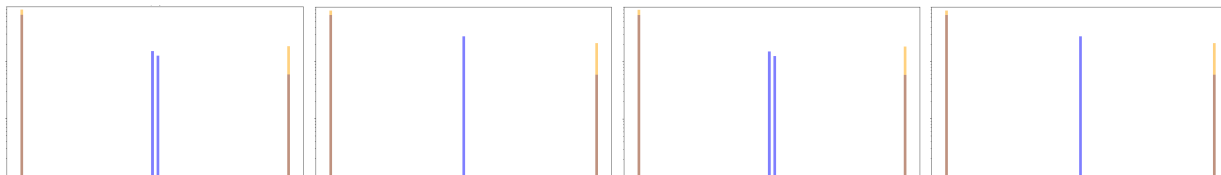


Figure 1: Histogram over Training Dataset of Four Consecutive Iterations (#47 – #50) of the DRO Formulation in Section 2.3 with $\{0, 1\}$ Loss of DNF Models. Horizontal axis is over Loss values in $[0, 1]$ and Vertical Axis provides Histogram Counts of datapoints. Experiments were over the ‘Heart’ instance; DRO Constraints of $\rho = 0.05$ Measured by χ^2 -distances were Imposed, and all $h_n \in \mathcal{H}$ satisfy $\mathfrak{C} \leq 5$.

Figure 1 plots in orange histograms of the instantaneous losses $l(h_n(x_i), y_i)$ observed for the n -th iterate h_n over the datapoints (indexed by i) in the training dataset for $n = 47, 48, 49$ and 50 . The experiments were conducted for the ‘heart’ problem instance, and DNF models with complexity $\mathfrak{C} \leq 5$ were considered. Since losses l are binary, this gives us a two-bin histogram in each iteration, with bins at loss values 0 and 1. Additionally provided in blue are histograms of the observed running average loss values at the data points: $(1/n) \sum_{j=1}^n l(h_j(x_i), y_i)$. The histograms of the average values are instructive in that they show identical histograms in every other iteration, which indicates that the chosen DNF iterates h_n flip the instantaneous loss values of a handful of datapoints and leaves the vast majority unchanged. This leads to a roughly equal split of the dataset into three subsets, the first where no chosen h_n iterate can classify the datapoints correctly (and so has an average loss of 1), the second where all chosen h_n iterates classify the points correctly (with an average loss of 0), and the third set where alternate iterates flip the correct/incorrect classification (leading to an average loss of ≈ 0.5). These results illustrate why the DRO philosophy of training continuously valued parameter models is of limited direct use when the models can produce only binary $\{0, 1\}$ loss information.

4.2 Comparisons of Parameter Settings

This section expands on the performance of the DR algorithm. We present a number of tables documenting the results of numerical experiments where specific parameters of the algorithm are varied. In each table presented below, we present two sets of columns each for the classification performance over unseen test data, the complexity of models constructed and the run length (number of iterations n) of the DR method. The first column is the results of the DR method with hyperparameters as presented in Table 1, and the results of the second column are obtained by changing one hyperparameter at a time. All Results are presented with a Mean and a 95% Confidence Interval, and the result with the best mean performance value among the two columns are highlighted in **bold**.

Table 2: Sparse Ensembles Constructed from Low ($\mathfrak{C}' = 5$) Complexity DNF Models are Compared to Ensembles Constructed from Moderate ($\mathfrak{C}' = 10$) Complexity DNF Models.

Dataset Name	Test Performance (%) of DR		Model Complexity of DR		n , number of Iterates of DR	
	$\mathfrak{C}' = 5$	$\mathfrak{C}' = 10$	$\mathfrak{C}' = 5$	$\mathfrak{C}' = 10$	$\mathfrak{C}' = 5$	$\mathfrak{C}' = 10$
heart	81.5 (1.7)	79.9(1.7)	26.0 (2.7)	30.0(0.0)	35.7 (3.6)	37.1(3.4)
ILPD	69.1(1.1)	69.8 (0.8)	13.3 (2.3)	30.0(0.0)	27.0 (1.8)	33.9(3.5)
FICO	72.1 (0.3)	71.5(0.3)	25.0 (2.5)	30.0(0.0)	33.9(3.3)	28.4 (2.0)
ionosphere	93.3 (1.4)	92.8(0.9)	20.3 (2.9)	30.0(0.0)	38.9 (4.0)	39.6(2.3)
liver	58.6 (1.6)	55.6(2.0)	29.3 (1.4)	30.0(0.0)	38.5(3.2)	34.4 (2.8)
pima	74.6 (1.4)	72.9(0.9)	25.0 (2.8)	30.0(0.0)	34.5 (3.6)	35.9(3.8)
transfusion	78.4 (0.8)	77.5(0.8)	14.3 (1.3)	29.0(1.3)	30.2(3.1)	27.6 (0.8)
WDBC	95.5(0.5)	95.6 (0.5)	28.3 (1.9)	30.0(0.0)	36.8 (3.9)	36.9(2.7)

The results presented in Table 2 contrast the ensembling of DNF models with a low value for $\mathfrak{C}' = 5$ to ensembling models with double the complexity $\mathfrak{C}' = 10$. All other parameters are held to their value used in Table 1: $P = P^0$ in the ensembling formulation (11), \mathfrak{C} is cutoff at 30, the DRO formulation (5) sets $\rho = 0.05$, and the outer iterations stop when no progress is made in 20 consecutive iterations. From the results, it is clear that the low complexity DNF models grant more generalization flexibility to the sparse ensembling formulation (10), beating the best ensembles assembled from $\mathfrak{C}' = 10$ in six of the eight cases (and significantly so, for example the ‘liver’ instance) and is within the 95% confidence interval of the best in all cases. Moreover, the total model complexity \mathfrak{C} produced for $\mathfrak{C}' = 5$ ensembles are significantly smaller in all instances. The generalization guarantee provided by Proposition 2 anticipates this, since it predicts that performance may degrade as \mathfrak{C}' increases.

Table 3: Aggregate Complexity of Sparse Ensemble Determined by (11) with a Cutoff at $\mathfrak{C} \leq 30$ Compared to a Cutoff at $\mathfrak{C} \leq 60$

Dataset Name	Test Performance (%) of DR		Model Complexity of DR		n , number of Iterates of DR	
	cutoff = 30	cutoff = 60	cutoff = 30	cutoff = 60	cutoff = 30	cutoff = 60
heart	81.5(1.7)	82.2 (1.7)	26.0 (2.7)	36.0(5.0)	35.7 (3.6)	38.7(3.7)
ILPD	69.1 (1.1)	69.1 (1.1)	13.3 (2.3)	13.3 (2.3)	27.0 (1.8)	27.0 (1.8)
FICO	72.1(0.3)	72.2 (0.3)	25.0 (2.5)	33.8(5.0)	33.9 (3.3)	38.1(3.7)
ionosphere	93.3 (1.4)	93.3 (1.4)	20.3 (2.9)	20.3 (2.9)	38.9 (4.0)	38.9 (4.0)
liver	58.6(1.6)	59.3 (1.3)	29.3 (1.4)	47.0(5.)	38.5 (3.2)	42.1(3.4)
pima	74.6 (1.4)	74.5(1.4)	25.0 (2.8)	30.3(3.7)	34.5 (3.6)	35.5(3.6)
transfusion	78.4 (0.8)	78.4 (0.8)	14.3 (1.3)	14.3 (1.3)	30.2 (3.1)	30.2 (3.1)
WDBC	95.5(0.5)	95.7 (0.5)	28.3 (1.9)	33.8(4.0)	36.8 (3.9)	38.2(3.6)

Table 3 varies the cutoff allowed in the inner sparse ensembling iterations where \mathfrak{C} is increased as $\mathfrak{C} = m \cdot \mathfrak{C}'$, $m = 1, 2, \dots$. The results presented in Table 1 above cuts off at $\mathfrak{C} \leq 30$ or earlier, which is compared to a larger cutoff of 60. Other parameters are held the same as in Table 1: $\mathfrak{C}' = 5$, the formulation (11) uses $P = P^0$, the DRO formulation (5) sets $\rho = 0.05$, and outer iterations stop when 20 consecutive iterations do not improve the training performance. As can be expected, the higher cutoff slightly improves the generalization performance, but this is at the expense of significantly more complex (and harder to interpret) models. Overall the cutoff of 30 appears to be preferable from the view of all three factors of good generalization performance at a low computational cost while producing models with good interpretability.

Table 4 presents another illustration of the better generalization of the ensembles constructed by the DR

method than the DNF models produced by the CG method. Test performance of the CG and DR methods are provided where the total complexity budget \mathfrak{C} is kept fixed to the value determined by the DR method when run with the settings that produced the results in Table 1. In every case, we observe that the test performance produced by the DR method exceeds (by a considerable margin in some cases) that produced by the CG method. Proposition 1 states that the DNF models produced by the CG method may suffer generalization error that is larger than the training error by a $O(\sqrt{\mathfrak{C}})$ term. So, while the DNF models have lower training error with the higher \mathfrak{C} budget, they will generalize less well. This is also attested to by the best model complexity chosen for CG with cross-validation as presented in Table 1: the average complexity is smaller than that of the DR output in nearly every case (though statistically identical for the ILPD dataset) and each is indeed closer to the complexity $\mathfrak{C}' = 5$ of the models that are aggregated by the DR method. On the other hand, by virtue of the generalization bound in Proposition 2, an ensemble of models produced by DR can reduce training error while still enjoying test performance within an $O(\sqrt{\mathfrak{C}'})$ term.

Table 4: Results for CG when Complexity Observed in DR Results are Imposed as Constraints on CG

Dataset Name	Test Performance (%)	
	DR	CG
heart	81.5 (1.7)	77.4(1.4)
ILPD	69.1 (1.1)	68.7(1.4)
FICO	72.1 (0.3)	70.9(0.3)
ionosphere	93.3 (1.4)	88.4(1.2)
liver	58.6 (1.6)	55.1(1.7)
pima	74.6 (1.4)	71.7(1.3)
transfusion	78.4 (0.8)	77.5(0.7)
WDBC	95.5 (0.5)	93.2(0.8)

Acknowledgements

We thank Alex Gray for suggesting the problem and the potential benefits of combining DRO and column generation to address the problem.

References

- Blanchet, J., Kang, Y., and Murthy, K. (2019a). Robust wasserstein profile inference and applications to machine learning. *Journal of Applied Probability*, 56(3):830–857.
- Blanchet, J. H., Kang, Y., Zhang, F., and Hu, Z. (2019b). A distributionally robust boosting algorithm. *2019 Winter Simulation Conference (WSC)*, pages 3728–3739.
- Breiman, L. (2001). Random forests. *Machine Learning*, 45:5–32.
- Breiman, L., Friedman, J. H., Olshen, R. A., and Stone, C. J. (1984). Classification and regression trees. *Biometrics*, 40:874.
- Dash, S., Gunluk, O., and Wei, D. (2018). Boolean decision rules via column generation. In Bengio, S., Wallach, H., Larochelle, H., Grauman, K., Cesa-Bianchi, N., and Garnett, R., editors, *Advances in Neural Information Processing Systems*, volume 31. Curran Associates, Inc.
- Dhurandhar, A., Shanmugam, K., and Luss, R. (2020). Enhancing simple models by exploiting what they already know. In *Proceedings of the 37th International Conference on Machine Learning, ICML’20*. JMLR.org.

- FICO (2018). FICO explainable machine learning challenge. <https://community.fico.com/community/xml>. Last accessed 2018-05-16.
- Freund, Y. and Schapire, R. E. (1997). A decision-theoretic generalization of on-line learning and an application to boosting. *Journal of Computer and System Sciences*, 55(1):119–139.
- Friedman, J., Hastie, T., and Tibshirani, R. (2000). Additive logistic regression: a statistical view of boosting (With discussion and a rejoinder by the authors). *The Annals of Statistics*, 28(2):337 – 407.
- Friedman, J. H. and Popescu, B. E. (2008). Predictive learning via rule ensembles. *Annals of Applied Statistics*, 2(3):916–954.
- Ghosh, S., Squillante, M. S., and Wollega, E. (2021). Efficient generalization with distributionally robust learning. In Ranzato, M., Beygelzimer, A., Dauphin, Y., Liang, P., and Vaughan, J. W., editors, *Advances in Neural Information Processing Systems*, volume 34, pages 28310–28322. Curran Associates, Inc.
- Golea, M., Bartlett, P., Lee, W. S., and Mason, L. (1997). Generalization in decision trees and dnf: Does size matter? In Jordan, M., Kearns, M., and Solla, S., editors, *Advances in Neural Information Processing Systems*, volume 10. MIT Press.
- Hu, X., Rudin, C., and Seltzer, M. (2019). Optimal sparse decision trees. In *Advances in Neural Information Processing Systems (NeurIPS)*.
- Lakkaraju, H., Bach, S. H., and Leskovec, J. (2016). Interpretable decision sets: A joint framework for description and prediction. In *Proceedings of the 22nd ACM SIGKDD International Conference on Knowledge Discovery and Data Mining*, KDD '16, page 1675–1684.
- Lam, H. and Zhou, E. (2017). The empirical likelihood approach to quantifying uncertainty in sample average approximation. *Operations Research Letters*, 45(4):301–307.
- Lichman, M. (2013). UCI machine learning repository.
- Luenberger, D. G. (1969). *Optimization by Vector Space Methods*. John Wiley & Sons.
- Muggleton, S. H., Schmid, U., Zeller, C., Tamaddoni-Nezhad, A., and Besold, T. (2018). Ultra-strong machine learning: comprehensibility of programs learned with ilp. *Machine Learning*, 107:1119–1140.
- Namkoong, H. and Duchi, J. C. (2017). Variance-based regularization with convex objectives. In Guyon, I., Luxburg, U. V., Bengio, S., Wallach, H., Fergus, R., Vishwanathan, S., and Garnett, R., editors, *Advances in Neural Information Processing Systems 30*, pages 2971–2980. Curran Associates, Inc.
- Ribeiro, M. T., Singh, S., and Guestrin, C. (2016). "why should i trust you?": Explaining the predictions of any classifier. In *Proceedings of the 22nd ACM SIGKDD International Conference on Knowledge Discovery and Data Mining*, KDD '16, page 1135–1144.
- Rudin, C. (2019). Stop explaining black box machine learning models for high stakes decisions and use interpretable models instead. *Nat Mach Intell.*, 1(5):206—215.
- Rudin, C., Chen, C., Chen, Z., Huang, H., Semenova, L., and Zhong, C. (2022). Interpretable machine learning: Fundamental principles and 10 grand challenges. *Statist. Surv.*, 16:1–85.
- Schapire, R. E., Freund, Y., Bartlett, P., and Lee, W. S. (1998). Boosting the margin: A new explanation for the effectiveness of voting methods. *The Annals of Statistics*, 26(5):1651–1686.
- Schmid, U., Zeller, C., Besold, T., Tamaddoni-Nezhad, A., and Muggleton, S. H. (2017). How does predicate invention affect human comprehensibility? In *ILP 2016*.

Sollich, P. and Krogh, A. (1995). Learning with ensembles: How overfitting can be useful. In Touretzky, D., Mozer, M., and Hasselmo, M., editors, *Advances in Neural Information Processing Systems*, volume 8. MIT Press.

Wang, T., Rudin, C., Doshi-Velez, F., Liu, Y., Klampfl, E., and MacNeille, P. (2017). A bayesian framework for learning rule sets for interpretable classification. *Journal of Machine Learning Research*, pages 1–37.

A PROOFS OF THEORETICAL ANALYSIS

The DNF models $h \in \mathcal{H}$ produce binary output $h : x \rightarrow y \in \{0, 1\}$, where \mathcal{H} denotes the space of all DNF rule sets of interest. The data (x, y) follow the true (unknown) distribution P^t , and we are given only an N -sized sample dataset $\mathcal{S} = \{(x_n, y_n), n \in [N]\}$ generated from P^t , using the notation $[N] = \{1, \dots, N\}$. The empirical equal-weight probability mass function (pmf) on \mathcal{S} is denoted by P^0 . In the sequel, we use the shorthand \mathbb{E}_t and \mathbb{P}_t for \mathbb{E}_{P^t} and \mathbb{P}_{P^t} , respectively, and similarly \mathbb{E}_0 and \mathbb{P}_0 for \mathbb{E}_{P^0} and \mathbb{P}_{P^0} .

Size of \mathcal{H} . The finite set $\mathcal{H} = \mathcal{H}(\mathfrak{C})$ contains all the DNF terms of complexity at most \mathfrak{C} . There are $\binom{2d}{c}$ choices for conjunctions of size c , and the complexity cost of each such term is $c + 1$. Hence, each $h \in \mathcal{H}$ is constituted from conjunctions of up to size $\mathfrak{C} - 1$.

For the number of conjunctions of size c , we have the lower bound

$$\binom{2d}{c} = \frac{2d}{c} \cdot \frac{2d-1}{c-1} \cdots \frac{2d-c+1}{1} \geq \left(\frac{2d}{c}\right)^c.$$

Meanwhile, we obtain the corresponding upper bound

$$\binom{2d}{c} = \frac{2d}{c} \cdot \frac{2d-1}{c-1} \cdots \frac{2d-c+1}{1} \leq \frac{(2d)^c}{c!} \leq \left(\frac{2de}{c}\right)^c,$$

where the last inequality uses the fact that $\exp(c) = \sum_{j=0}^{\infty} c^j/j!$.

Since the number of conjunctions grows exponentially with c , there exists a constant $V > 1$ such that $|\mathcal{H}| \leq V \cdot \binom{2d}{\mathfrak{C}-1}$. To see this, consider the subset of \mathcal{H} with one term of size $c < \mathfrak{C} - 1$. Then, this subset is of size at most $\binom{2d}{c} \cdot (\mathfrak{C}-1-\binom{2d}{c+1}) \lll \binom{2d}{\mathfrak{C}-1}$. Thus, we also have that

$$(\mathfrak{C}-1) \log \frac{2d}{\mathfrak{C}-1} \leq \log |\mathcal{H}| \leq \log V + (\mathfrak{C}-1) \log \frac{2de}{\mathfrak{C}-1}. \quad (15)$$

A.1 Proposition 1: Generalization of DNF Models

We now establish the following proposition from the main body of the paper.

Proposition 1. *Let P^t be the underlying distribution and P^0 the empirical pmf over a training set \mathcal{S} of size N , and the loss is measured as $l(h(x), y) = |h(x) - y|$. Then, for any $\delta \in (0, 1)$, there exists constants such that for all rule sets h with max-complexity $c(h) \leq \mathfrak{C}$, we have with probability at least $1 - \delta$:*

$$\mathbb{E}_{P^t}[l(h(x), y)] \leq \mathbb{E}_{P^0}[l(h(x), y)] + \left(\frac{2}{N} \left((\mathfrak{C}-1) \log \frac{2d}{\mathfrak{C}-1} + \log \frac{1}{\delta} \right)\right)^{\frac{1}{2}}.$$

Proof. For the true (unknown) data distribution $(x, y) \sim P^t$ over the space of features and labels, let $p_h = \mathbb{P}_t(h(x) \neq y)$. Since both h and y are binary, the loss function $l(h(x), y) = |h(x) - y| = \mathbb{I}(h(x) \neq y)$. Define the random variable $Z_h = \mathbb{I}(h(x) \neq y)$ as a Bernoulli random variable with the probability of success (misclassification) p_h . The training dataset \mathcal{S} can also be viewed as a set of N independent draws of Bernoulli random variables Z_n , and $\hat{p}_{h,N} = \frac{1}{N} \sum_{n \in [N]} \mathbb{I}(Z_n = 1)$ is an N sample approximation of the probability p_h .

For each $h \in \mathcal{H}$, the right-tail Chernoff bound for Bernoulli random variables yields

$$\mathbb{P}(p_h - \hat{p}_{h,N} \geq \lambda) \leq \exp(-N\lambda^2/2),$$

where the probability is taken with respect to the sampling of \mathcal{S} from P_t . To obtain a uniform bound that applies to all $h \in \mathcal{H}$, we employ the union bound principle that $\mathbb{P}(\cup_i A_i) \leq \sum_i \mathbb{P}(A_i)$ for events A_i . Thus, we have

$$\mathbb{P}(\exists h \in \mathcal{H} \mid p_h - \hat{p}_{h,N} \geq \lambda) \leq |\mathcal{H}| \exp(-N\lambda^2/2).$$

Using the lower bound in (15), we obtain the desired generalization result when λ is set as

$$\lambda = \left(\frac{2}{N} \left((\mathfrak{C}-1) \log \frac{2d}{\mathfrak{C}-1} + \log \frac{1}{\delta} \right)\right)^{\frac{1}{2}}. \quad \square$$

A.2 Proposition 2: Generalization of Convex Combinations

We consider convex combination models of the form $F(x) = \sum_{h \in \mathcal{H}} v_h h(x)$, where the real-valued v_h are non-negative and $\sum_h v_h = 1$. The set representing misclassification by $F(x)$ is compactly written as

$$\left\{ \left(y - \frac{1}{2} \right) \left(F(x) - \frac{1}{2} \right) \leq 0 \right\} \iff \left\{ F(x) \leq \frac{1}{2}, y = 1 \right\} \cup \left\{ F(x) > \frac{1}{2}, y = 0 \right\}.$$

Define $L(f, x, y) := (y - 1/2)(f(x) - 1/2)$. We wish to obtain a bound on $\mathbb{P}_t(L(F, x, y) \leq 0)$ in terms of the corresponding probability under the empirical pmf P^0 . The next result provides a bound on the generalization performance of such convex models. Note that, since the v_h are real-valued, any uniform bound on the worst performance of *any* F cannot be stated as cleanly as in Proposition 1. We introduce an additional parameter $\Delta > 0$ in the following proposition from the main body of the paper, which we now establish.

Proposition 2. *For any convex rule set combination $F = \sum_k v_k h_k$, define $\mathfrak{C}' := \max_k \{c(h_k)\}$ to be the maximum complexity of its constituent conjunctive terms, and let the predicted label be $\hat{y} = \mathbb{I}(F(x) \geq 1/2)$. Then, for any given $\delta \in (0, 1)$, with probability at least $1 - \delta$, we have*

$$\mathbb{P}_t(L(F, x, y) \leq 0) \leq \mathbb{P}_0(L(F, x, y) \leq \Delta) + O\left(\frac{1}{\sqrt{N}} \left(\frac{(\mathfrak{C}' - 1)}{\Delta^2} \log N + \log \frac{1}{\delta} \right)^{1/2}\right).$$

The parameter Δ plays an important role in the analysis of generalization as presented in Proposition 2. The upper bound described above becomes increasingly lax as $\Delta \searrow 0$. It is not merely a convenient device to ease the construction of the rigorous guarantee, but it also has an important practical implication in the sparse ensembling formulation (11). Our experiments show that the Δ in this formulation, which plays the same role as in Proposition 2, must be a small positive value for the optimal sparse convex combinations identified by the formulation to be of higher generalization power than the individual DNF models.

Proof of Proposition 2.

Let us start by noting that the set of convex weights $\{v_h, h \in \mathcal{H} = \mathcal{H}(\mathfrak{C}')\}$ themselves represent a pmf. The analysis of the generalization error of F utilizes this fact and approximates F using an M -sized collection of DNFs sampled from (v_h) , as introduced by Schapire et al. (1998). Define the approximation set

$$\mathcal{G}_M := \left\{ g : x \rightarrow \left\{ 0, \frac{1}{M}, \dots, 1 \right\} \mid g(x) = \frac{1}{M} \sum_{m \in [M]} h_m(x), \text{ where } h_m \in \mathcal{H}(\mathfrak{C}') \ \forall m \in [M] \right\}.$$

(We will specify the right size M to use later in the proof.) Note that $|\mathcal{G}_M| = |\mathcal{H}|^M$. The analysis of $g \in \mathcal{G}_M$ is easier than F directly because g only takes values in the lattice $\{0, 1/M, 2/M, \dots, 1\}$. Let \mathcal{V} be the distribution induced on \mathcal{G}_M by sampling the components of a $g \in \mathcal{G}_M$ from the pmf formed from the coefficients (v_h) of F . Our main result is established in two steps. In the first step, we start by uniformly bounding the probability of the misclassification event $\{L(F, x, y) \leq 0\}$ of F under the true distribution P^t with the probability that $L(g, x, y) \leq \Delta/2$ under the empirical pmf P^0 for an *arbitrarily* chosen $g \in \mathcal{G}_M$ that is sampled from the distribution \mathcal{V} . We then bound the latter with the probability that $L(F, x, y) \leq \Delta$ under the same empirical pmf P^0 .

Let $A = \{L(F, x, y) \leq 0\}$ and $B = \{L(g, x, y) \leq \Delta/2\}$, where g is any (fixed) element from \mathcal{G}_M and $\Delta > 0$ is an arbitrary constant. Then, by the law of total probability and the definition of conditional probability, we have that $\mathbb{P}_t A = \mathbb{P}_t[A \cap B] + \mathbb{P}_t[A \cap B^c] = \mathbb{P}_t[A|B] \mathbb{P}_t B + \mathbb{P}_t[B^c|A] \mathbb{P}_t A \leq \mathbb{P}_t B + \mathbb{P}_t[B^c|A]$. Thus, we conclude

$$\mathbb{P}_t(L(F, x, y) \leq 0) \leq \mathbb{P}_t\left(L(g, x, y) \leq \frac{\Delta}{2}\right) + \mathbb{P}_t\left(L(g, x, y) > \frac{\Delta}{2} \mid L(F, x, y) \leq 0\right).$$

Since this applies to any $g \in \mathcal{G}_M$, we can take expectations on the right hand side with respect to the distribution \mathcal{V} on \mathcal{G}_M to obtain that

$$\mathbb{P}_t(L(F, x, y) \leq 0) \leq \mathbb{E}_{\mathcal{V}} \left[\mathbb{P}_t \left(L(g, x, y) \leq \frac{\Delta}{2} \right) \right] + \mathbb{E}_t \left[\mathbb{P}_{\mathcal{V}} \left(L(g, x, y) > \frac{\Delta}{2} \mid L(F, x, y) \leq 0 \right) \right]. \quad (16)$$

We shall bound in turn the inner probability terms within the expectations of each summand on the right hand side of (16). For the first summand, we treat the g as a fixed sum of DNF terms, and thus apply the same union bound analysis from the proof of Proposition 1 to the Bernoulli random variable $\mathbb{I}\left(L(g, x, y) \leq \frac{\Delta}{2}\right)$.

This yields that the probability (over the sampling of \mathcal{S} from P^t) that there exists at least one g and $\Delta > 0$ for which

$$\mathbb{P}_t\left(L(g, x, y) \leq \frac{\Delta}{2}\right) > \mathbb{P}_0\left(L(g, x, y) \leq \frac{\Delta}{2}\right) + \lambda_M \quad (17)$$

is at most

$$(M+1)|\mathcal{H}|^M \exp(-2N\lambda_M^2).$$

The term $\exp(-2N\lambda_M^2)$ comes from the Chernoff bound for *any* fixed g and Δ . There are $|\mathcal{G}_M| = |\mathcal{H}|^M$ such g over which to take the union. Moreover, each $g \in \mathcal{G}_M$ takes one of only $M+1$ distinct values $\{0, 1/M, \dots, 1\}$, and there are at most $(M+1)|\mathcal{H}|^M$ combinations of g and Δ to consider. Hence, for any fixed M , we proceed as in the proof of Proposition 1 to set

$$\lambda_M = \left(\frac{1}{2N} \log\left(\frac{(M+1)|\mathcal{H}|^M}{\delta_M}\right)\right)^{\frac{1}{2}}, \quad (18)$$

and thus obtain that, with at least probability $1 - \delta_M$, the bound in (17) is satisfied for *every* g and Δ . Taking the expectation needed in (16) with respect to the distribution \mathcal{V} , we have with probability $1 - \delta_M$ that

$$\mathbb{P}_{t,\mathcal{V}}\left(L(g, x, y) \leq \frac{\Delta}{2}\right) \leq \mathbb{P}_{0,\mathcal{V}}\left(L(g, x, y) \leq \frac{\Delta}{2}\right) + \lambda_M.$$

To complete the analysis of this first summand of (16), we need to provide an upper bound for the first term on the right hand side of the above expression. Utilizing the same conditioning argument that led to (16), we can write that

$$\mathbb{P}_{0,\mathcal{V}}\left(L(g, x, y) \leq \frac{\Delta}{2}\right) \leq \mathbb{P}_0\left(L(F, x, y) \leq \Delta\right) + \mathbb{E}_0\left[\mathbb{P}_{\mathcal{V}}\left(L(F, x, y) > \Delta \mid L(g, x, y) \leq \frac{\Delta}{2}\right)\right]. \quad (19)$$

Here, the F in the first term on the right hand side is unaffected by the distribution \mathcal{V} of $g \in \mathcal{G}_M$. The probability inside the expectation in the second term is similar in spirit to that of the second summand in (16) and deals with the sampling of $g \in \mathcal{G}_M$ from the induced distribution \mathcal{V} . Note that $F(x) = \mathbb{E}_{\mathcal{V}}g(x)$ and the pmf (v_h) from which the $g(x) \sim \mathcal{V}$ is sampled has finite support of size $|\mathcal{H}|$. This allows us to exploit the Chernoff bound for finite support distributions. In particular, for the second term in (19), we obtain that

$$\mathbb{P}_{\mathcal{V}}\left(L(F, x, y) > \Delta \mid L(g, x, y) \leq \frac{\Delta}{2}\right) \leq \exp\left(-\frac{M\Delta^2}{8}\right). \quad (20)$$

For the second summand in (16), we analogously have

$$\mathbb{P}_{\mathcal{V}}\left(L(g, x, y) > \frac{\Delta}{2} \mid L(F, x, y) \leq 0\right) \leq \exp\left(-\frac{M\Delta^2}{8}\right). \quad (21)$$

Upon combining (16), (17), (19), (20) and (21), we have established, for an arbitrary M and with probability at least $1 - \delta_M$, that

$$\mathbb{P}_t(L(F, x, y) \leq 0) \leq \mathbb{P}_0\left(L(F, x, y) \leq \Delta\right) + 2 \exp\left(-\frac{M\Delta^2}{8}\right) + \lambda_M, \quad (22)$$

where λ_M is as chosen in (18). To obtain a bound that applies uniformly for *any* M , we once again appeal to the union bound analysis by setting $\delta_M = \delta\left(\frac{1}{M} - \frac{1}{M+1}\right)$. Thus, with probability at least $1 - \sum_{M \geq 1} \delta_M = 1 - \delta$, we have that the bound in (22) is uniformly satisfied for any $M \geq 1$.

There are two terms that depend on M in the right side of (22). The middle term exponentially decreases with M , while λ_M (with form given in (18) after substituting δ_M) has a leading term that increases as a small polynomial of M . In order to strike a balance between these terms, we choose a value for M by setting $\exp(-M\Delta^2/8) = \sqrt{\log |\mathcal{H}|/N}$. Thus, we obtain

$$M = \frac{4^2}{\Delta} \log \left(\frac{N}{\log |\mathcal{H}(\mathcal{C}')|} \right).$$

Further, using the lower bound on $\log |\mathcal{H}(\mathcal{C}')|$ from (15) yields the desired result. \square

B COLUMN GENERATION FOR (4)

The size of the set K in the formulation to search over the space of rule sets $\mathcal{H}(\mathcal{C}')$ clearly grows as an exponential function of the number of binary features. Solving IPs with exponentially many variables is impractical; even the associated LP relaxation is hard to solve. Notice that the number of constraints (that are not variable constraints) in this formulation is bounded by the number of data points with label 1. One approach to solving large LPs that have few constraints but very many variables is to use *column generation*. This approach is motivated by the following: (1) there is a solution to the LP in which the number of nonzero variable values is bounded above by the number of constraints; (2) when solving the LP relaxation with the simplex method, it is fairly common that the total number of variables that are ever set to nonzero values in intermediate steps is a small multiple of the number of constraints. In other words, only a small subset of all possible w_k variables (rules) is generated explicitly and the optimality of the LP is guaranteed by iteratively solving a *pricing problem* that implicitly checks the dual constraints.

To apply this framework to the IP (which we refer to as the “master IP” or MIP, with associated LP relaxation denoted by “master LP” or MLP), we first replace K with a very small subset of its elements and explicitly solve the LP relaxation of the resulting smaller problem, which we call the *Restricted master LP* or RMLP. Any optimal solution of RMLP can be extended to a solution of MLP with the same objective value by setting all missing w_k variables to zero; this solution provides an upper bound on the optimal solution value of MLP. One can potentially improve such a solution by augmenting RMLP with additional variables corresponding to some of the missing rules. The second step is to identify such rules without explicitly considering all of them. Repeating these steps until there are no improving rules (i.e., variables missing from the Restricted MLP that can reduce the cost) solves the MLP to optimality.

To find the missing improving rules, one needs to check for variables in MLP missing from RMLP that have negative reduced cost (with respect to the dual solution from RMLP applied to variables in MLP not present in RMLP). The reduced cost of a missing variable (or variable set to zero in MLP) gives the maximum possible change in objective value per unit increase in that variable’s value. Therefore, if all missing variables from RMLP have non-negative reduced cost, then the optimal solution for RMLP yields an optimal solution of MLP. Furthermore, missing variables that have large negative reduced costs are more likely to improve the objective value of RMLP. We next formulate an optimization problem that uses the optimal dual solution of RMLP and checks for negative reduced cost columns in MLP. Let $\mu_i \geq 0$ denote the dual variable associated with constraint (7) corresponding to the i th data point with label 1. Let $\lambda \geq 0$ be the dual variable associated with the complexity bound constraint. Let $\delta_i \in \{0, 1\}$ denote whether the i th sample satisfies rule k . Recall that c_k is the complexity of rule k ; then its reduced cost is equal to

$$\sum_{i:y_i=0} P_i \delta_i - \sum_{i:y_i=1} P_i \mu_i \delta_i + \lambda c_k. \quad (23)$$

The first term in (23) is the cost of rule k in the objective function (6), expressed in terms of δ_i . The second term is the sum of the dual variables associated with constraints (7). The last term is the dual variable associated with the complexity constraint multiplied by the complexity of rule k .

We now formulate an IP to express rules as conjunctions of the original features. Let the decision variable $z_j \in \{0, 1\}$ denote if feature j is selected in the rule. Let S_i correspond to the zero-valued features in sample

i. Let J be the index set of all features. Then the *Pricing Problem* below identifies the rule k missing from RMLP that has the lowest reduced cost.

$$z_{CG} = \mathbf{min} \quad \lambda \left(1 + \sum_{j \in J} z_j \right) - \sum_{i: y_i=1} P_i \mu_i \delta_i + \sum_{i: y_i=0} P_i \delta_i \quad (24)$$

$$\mathbf{s.t.} \quad \delta_i + z_j \leq 1, \quad j \in S_i, \forall i : y_i = 1 \quad (25)$$

$$\delta_i \geq 1 - \sum_{j \in S_i} z_j, \quad \delta_i \geq 0, \quad \forall i : y_i = 0 \quad (26)$$

$$\sum_{j \in J} z_j \leq c, \quad (27)$$

$$z_j \in \{0, 1\}, \quad j \in J. \quad (28)$$

The first term in (24) expresses the complexity c_k in terms of the number of selected features. Constraints (25), (26) ensure that the rule acts as a conjunction, i.e., it is satisfied ($\delta_i = 1$) only if no zero-valued features are selected ($z_j = 0$ for $j \in S_i$). Similar to ξ_i in MIP, the variables δ_i do not have to be explicitly defined as binary due to the objective function. Constraint (27) bounds the number of features allowed in any rule.

The optimal solution to the Pricing Problem above gives the rule with the minimum reduced cost that is missing from RMLP. The reduced cost of this rule equals z_{CG} and if $z_{CG} < 0$, then the corresponding variable is added to RMLP. More generally, any feasible solution to the Pricing Problem that has a negative objective function value gives a rule with a negative reduced cost and therefore can be added to RMLP to improve its value.

C SOLVING DRO FORMULATION (5)

We now present an algorithm due to Ghosh et al. (2021) that is adapted in this paper to solve the DRO formulation (5) for the worst-case pmf. Recall that the formulation (5) can be equivalently written as the concave problem given in (9), where the objective function of (5) is expressed as $\sum_{i \in [N]} l(F_n(x_i), y_i) \cdot P_i$ and the individual loss values $z_i = l(F_n(x_i), y_i)$ are constructed as per (2) taking values in the discrete set $\{0, 1/n, \dots, 1\}$. The Lagrangian objective of (9) can be expressed as

$$\mathcal{L}(\alpha, \lambda, P) = \sum_{i \in \mathcal{S}} P_i z_i + \lambda \left(1 - \sum_{i \in \mathcal{S}} P_i \right) + \frac{\alpha}{N} \left(N\rho - \sum_{i \in \mathcal{S}} \Phi(NP_i) \right). \quad (29)$$

From optimization theory (Luenberger, 1969), this leads to the optimal objective value of (9) given by $\tilde{R}^*(F_n) = \min_{\alpha \geq 0, \lambda} \max_{P_i \geq 0} \mathcal{L}(\alpha, \lambda, P)$. We then solve the Lagrangian formulation in (29) for a given iteration n using Algorithm 1, adapted from (Ghosh et al., 2021), to obtain a feasible primal-dual solution $(P^*, \alpha^*, \lambda^*)$ to (9) with an objective value \tilde{R}^* such that $|R^*(F_n) - \tilde{R}^*| < \epsilon$ according to Proposition 3.

D DETAILS ON NUMERICAL EXPERIMENTS

The datasets were pre-processed as described by Dash et al. (2018). We used the standard “dummy”/“one-hot” coding to transform categorical features into multiple binary features. Each category is represented by two binary features, one indicating the presence of that category and one indicating the absence of that category. The non-binary numerical features are transformed into a sequence of binary features where each feature represents the satisfaction or not of a certain threshold and its negation. As an example, for a certain numerical feature X , we could create the features $X \leq 1$, $X \leq 2$ and $X > 1$, $X > 2$. The thresholds used were deciles computed from the samples.

Two of the UCI repository datasets were slightly modified as follows:

Algorithm 1 Robust Loss Maximization

Given: loss values $\mathcal{Z} = \{z_1, \dots, z_N\}$; dataset support indices $[N] = \{1, \dots, N\}$; D_ϕ constraint ρ .

1. *Case:* $\alpha^* = 0$ along with constraint $D_\phi(P^*, P^0) \leq \rho$.
 - (a) Let $\mathcal{N} = \{i \in [N] : z_i = \max_{j \in [N]} z_j\}$. Set $\alpha^* = 0$ in (29), and then an optimal solution is P^* where $P_i^* = \frac{1}{|\mathcal{N}|}$, $\forall i \in \mathcal{N}$, and $P_i^* = 0$, $\forall i \notin \mathcal{N}$.
 - (b) If $D_\phi(P^*, P^0) \leq \rho$, then **stop** and return P^* .
2. *Case:* constraint $D_\phi(P^*, P^0) = \rho$ with $\alpha^* \geq 0$.
 - (a) Keeping λ, α fixed, solve for the optimal P^* (as a function of λ, α) that maximizes $\mathcal{L}(\alpha, \lambda, P)$, applying the constraint $P_i \geq 0$.
 - (b) Keeping α fixed, solve for the optimal λ^* using the first order optimality condition on $\mathcal{L}(\alpha, \lambda, P^*)$. Note that this is equivalent to satisfying the equation $\sum_{i \in [N]} P_i^* = 1$. The proof of Proposition 3 (Ghosh et al., 2021) shows that this step is at worst a bisection search in one dimension, but in some cases (e.g., KL-divergence) a solution λ^* is available in closed form. The proof of Proposition 3 also provides finite bounds $[\underline{\lambda}, \bar{\lambda}]$ on the range over which we need to search for λ^* .
 - (c) Apply the first order optimality condition to the one-dimensional function $\mathcal{L}(\alpha, \lambda^*(\alpha), P^*)$ to obtain the optimal $\alpha^* \geq 0$. This is equivalent to requiring that α^* satisfies the equation $\sum_{i \in [N]} \phi(P_i^*) = \rho$. The proof of Proposition 3 (Ghosh et al., 2021) shows that this is at worst a one-dimensional bisection search which embeds the previous step in each function call of the search.
 - (d) Let $\phi'(s) = d\phi(s)/ds$ denote the derivative of $\phi(s)$ with respect to s , and $(\phi')^{-1}$ its inverse. Define the index set $\mathcal{N} := \{i \in [N] \mid \lambda^* \leq z_i - \alpha^* \phi'(0)\}$, with $\mathcal{N} = \emptyset$ if $\phi'(s) \rightarrow -\infty$ as $s \rightarrow 0+$. Set

$$P_i^* = \begin{cases} \frac{1}{N} (\phi')^{-1} \left(\frac{z_i - \lambda^*}{\alpha^*} \right), & i \in \mathcal{N} \\ 0 & i \notin \mathcal{N} \end{cases}. \quad (30)$$

Return P^* .

- For the ‘liver’ dataset, we used the number of drinks as the output variable instead of the selector variable. The number of drinks Y was represented by the two features $Y \leq 2$ and $Y > 2$.
- For the ‘heart’ dataset, we used only the Cleveland data and removed 4 samples with ‘ca’ = ?, yielding 299 samples. The label was binarized as either $X = 0$ or $X > 0$.

The FICO dataset was also slightly modified due to missing values and the presence of special values. The 588 records that only contain missing values (represented by -9) were removed. Entries meaning ‘no inquiries or delinquencies observed’ (represented by -7) were replaced by the maximum number of elapsed months in the data plus 1. The remaining missing values (represented by -9) and entries meaning ‘not applicable’ (represented by -8) were combined into a single null category. During binarization, a special indicator was created for these null values and all other comparisons with the null value return False. Values greater than 7 (other) in ‘MaxDelq2PublicRecLast12M’ were imputed as 7 (current and never delinquent) based on the corresponding values in ‘MaxDelqEver’.

This section expands on the performance of the DR (Distributionally robust Rule sets) algorithm. We present a number of tables documenting the results of numerical experiments where specific parameters of the algorithm are varied. In each table presented below, we present two sets of columns each for the classification performance over unseen test data, the complexity of models constructed and the run length (number of iterations n) of the DR method. The first column is the results of the DR method with hyperparameters as

presented in Table 1, and the results of the second column are obtained by changing one hyperparameter at a time. All Results are presented with a Mean and a 95% Confidence Interval, as in the main body of the paper. The result with the best mean performance value among the two columns are highlighted in **bold**.

Table 5: Data Weights P in the Sparse Ensembling Formulation (11) are varied between the Empirical PMF P^0 and the DRO-identified Worst Weights P^n from (5)

Dataset Name	Test Performance (%) of DR		Model Complexity of DR		n , number of Iterates of DR	
	P^0	P^n	P^0	P^n	P^0	P^n
heart	81.5(1.7)	81.9 (1.5)	26.0(2.7)	25.3 (2.6)	35.7 (3.6)	37.6(4.0)
ILPD	69.1(1.1)	69.6 (1.0)	13.3 (2.3)	15.3(2.4)	27.0 (1.8)	28.4(2.1)
FICO	72.1 (0.3)	71.9(0.3)	25.0 (2.5)	27.8(2.0)	33.9 (3.3)	36.2(3.3)
ionosphere	93.3 (1.4)	93.1(1.2)	20.3(2.9)	17.3 (2.0)	38.9(4.0)	38.0 (3.4)
liver	58.6 (1.6)	58.6 (1.3)	29.3(1.4)	28.3 (1.9)	38.5 (3.2)	39.9(3.2)
pima	74.6 (1.4)	73.8(1.2)	25.0(2.8)	21.3 (3.3)	34.5 (3.6)	37.0(3.7)
transfusion	78.4(0.8)	78.6 (0.9)	14.3 (1.3)	14.3 (2.5)	30.2(3.1)	29.9 (2.8)
WDBC	95.5 (0.5)	95.4(0.6)	28.3(1.9)	25.3 (2.9)	36.8(3.9)	35.4 (3.4)

Table 5 analyzes the sensitivity of the sparse ensembling formulation (11) to the data weights P used. We specifically compare the setting of these weights to the empirical pmf ($P = P^0$) with the setting of these weights to the current worst-case pmf ($P = P^n$) identified by the n -th iteration of the DRO formulation (5). All other parameters are held to their value used in Table 1: $\mathcal{C}' = 5$, \mathcal{C} is cutoff at 30, the DRO formulation (5) sets $\rho = 0.05$, and the stopping criterion of the outer iteration waits to ensure no improvements are noticed in 20 consecutive iterations. The results establish that neither setting dominates the other, and so in our main results we use $P = P^0$. The P^n may not bring additional benefits in the ensembling formulation (11) because the impact of the worst-case weights are already encoded in the choice of the DNF iterates produced by the formulation (4) that determines the members of the collection of iterates among which the sparse ensemble is chosen.

Table 6: DRO Radius Parameter ρ is varied from 0.05 to 0.5

Dataset Name	Test Performance (%) of DR		Model Complexity of DR		n , number of Iterates of DR	
	$\rho = 0.05$	$\rho = 0.5$	$\rho = 0.05$	$\rho = 0.5$	$\rho = 0.05$	$\rho = 0.5$
heart	81.5(1.7)	81.6 (1.1)	26.0 (2.7)	29.5(1.0)	35.7 (3.6)	40.3(3.5)
ILPD	69.1(1.1)	69.3 (1.1)	13.3(2.3)	12.8 (1.8)	27.0(1.8)	26.3 (0.3)
FICO	72.1 (0.3)	71.4(0.3)	25.0(2.5)	20.8 (3.0)	33.9 (3.3)	35.3(3.2)
ionosphere	93.3 (1.4)	91.5(1.1)	20.3 (2.9)	30.0(0.0)	38.9 (4.0)	42.2(3.0)
pima	74.6 (1.4)	73.8(1.5)	25.0(2.8)	24.3 (3.5)	34.5 (3.6)	38.7(3.4)
transfusion	78.4(0.8)	78.6 (0.7)	14.3(1.3)	13.0 (1.3)	30.2(3.1)	26.9 (0.8)
WDBC	95.5 (0.5)	95.0(0.4)	28.3(1.9)	27.8 (2.0)	36.8(3.9)	36.3 (3.7)

In Table 6, results are presented for a larger DRO parameter $\rho = 0.5$, keeping all other parameters the same as in Table 1: $\mathcal{C}' = 5$, \mathcal{C} is cutoff at 30, the ensembling formulation (11) uses $P = P^0$, and iterations n stop after 20 consecutive iterations of little improvement. Recall that this parameter was set to match the recommendation of \mathcal{C}'/N from the DRO analysis of Namkoong and Duchi (2017) for continuous convex models. The results presented in Table 6 illustrate that $\rho = 0.05$ is on balance better than the larger $\rho = 0.5$ which may make the DRO formulation too conservative. (Note that, for the ‘liver’ instance, the setting of $\rho = 0.5$ was too large rendering overly conservative results, and thus such results are omitted.)

Table 7 varies the stopping criterion parameter of how many consecutive iterations of less than 0.5%

Table 7: Minimum Number of Consecutive Iterations of No-Improvement to Observe before Stopping Outer Iterations Indexed by n

Dataset Name	Test Performance (%) of DR			Model Complexity of DR			n , number of Iterates of DR		
	10	20	30	10	20	30	10	20	30
heart	81.5(1.7)	81.5(1.7)	81.6(1.7)	25.0(3.0)	26.0(2.7)	25.5(2.8)	21.2(2.0)	35.7(3.6)	44.2(2.3)
ILPD	69.1(1.1)	69.1(1.1)	69.2(1.1)	13.3(2.3)	13.3(2.3)	13.3(2.3)	16.2(0.3)	27.0(1.8)	36.8(1.3)
FICO	72.1(0.2)	72.1(0.3)	72.2(0.2)	25.0(2.9)	25.0(2.5)	26.5(2.1)	22.5(2.5)	33.9(3.3)	43.4(2.5)
ionosphere	93.1(1.4)	93.3(1.4)	93.2(1.4)	19.3(2.5)	20.3(2.9)	21.3(2.9)	22.4(2.5)	38.9(4.0)	46.0(2.2)
liver	58.7(1.4)	58.6(1.6)	58.2(1.8)	28.3(1.9)	29.3(1.4)	28.8(1.7)	26.4(2.4)	38.5(3.2)	46.8(1.7)
pima	74.6(1.2)	74.6(1.4)	74.3(1.3)	23.8(2.8)	25.0(2.8)	24.3(2.9)	22.2(2.4)	34.5(3.6)	43.4(2.5)
transfusion	78.5(0.7)	78.4(0.8)	78.4(0.8)	13.3(1.3)	14.3(1.3)	14.3(1.3)	17.4(2.1)	30.2(3.1)	39.6(2.5)
WDBC	95.4(0.6)	95.5(0.5)	95.6(0.5)	27.3(2.4)	28.3(1.9)	27.3(2.4)	21.3(1.6)	36.8(3.9)	44.7(2.3)

aggregate improvement (in training performance) to observe before terminating the outer iterations. We present results for this parameter being set at 10 and 30 and reproduce the results for 20 as presented in the main body of the paper. The other parameters are held at their previous values: $\mathcal{C}' = 5$, $\rho = 0.05$, and \mathcal{C} is cutoff at 30. The more aggressive parameter value of 10 can produce lower complexity models more quickly, while the more conservative setting of 30 can provide improvements in test performance at the expense of longer computation time and less interpretable models. The value of 20, chosen for the results presented in the main body, seems to attain a good balance over these three competing factors.